IAEA
International Atomic Energy Agency

20th IAEA Fusion Energy Conference
Vilamoura, Portugal, 1 to 6 November 2004

IAEA-CN-116/EX/P2-7

STATIONARY, HIGH BOOTSTRAP FRACTION PLASMAS IN DIII-D WITHOUT INDUCTIVE CURRENT CONTROL

P.A. POLITZER, A.W. HYATT, T.C. LUCE, F.W. PERKINS,[1] R. PRATER, A.D. TURNBULL, D.P. BRENNAN,[2] J.R. FERRON, C.M. GREENFIELD, R.J. JAYAKUMAR,[3] R.J. LA HAYE, E.A. LAZARUS,[4] C.C. PETTY, and M.R. WADE

General Atomics
San Diego, California 92186-5608
United States of America

[1]Princeton Plasma Physics Laboratory, Princeton, New Jersey, USA
[2]Massachusetts Institute of Technology, Cambridge, Massachusetts, USA
[3]Lawrence Livermore National Laboratory, Livermore, California, USA
[4]Oak Ridge National Laboratory, Oak Ridge, Tennessee, USA

Stationary, High Bootstrap Fraction Plasmas in DIII-D Without Inductive Current Control

P.A. Politzer,[1] A.W. Hyatt,[1] T.C. Luce,[1] F.W. Perkins,[2] R. Prater,[1] A.D. Turnbull,[1] D.P. Brennan,[3] J.R. Ferron,[1] C.M. Greenfield,[1] J. Jayakumar,[4] R.J. La Haye,[1] E.A. Lazarus,[3] C.C. Petty,[1] and M.R. Wade[5]

[1]General Atomics, P.O. Box 85608, San Diego, California, USA
[2]Princeton Plasma Physics Laboratory, Princeton, New Jersey, USA
[3]Massachusetts Institute of Technology, Cambridge, Massachusetts, USA
[4]Lawrence Livermore National Laboratory, Livermore, California, USA
[5]Oak Ridge National Laboratory, Oak Ridge, Tennessee, USA

email: politzer@fusion.gat.com

Abstract. We have initiated an experimental program to address some of the questions associated with operation of a tokamak with high bootstrap current fraction under high performance conditions, without assistance from a transformer. In these discharges stationary (or slowly improving) conditions are maintained for > 3.7 s at $\beta_N \approx \beta_p \leq 3.3$. The achievable current and pressure are limited by a relaxation oscillation, involving growth and collapse of an ITB at $\rho \geq 0.6$. The pressure gradually increases and the current profile broadens throughout the discharge. Eventually the plasma reaches a more stable, high confinement (H89P ~ 3) state. Characteristically these plasmas have 65%–85% bootstrap current, 15%–30% NBCD, and 0%–10% ECCD.

1. Introduction

Fully noninductive operation will be essential for eventual steady-state tokamak reactors. For efficient operation, the bootstrap current fraction must be close to 100%, allowing for a small additional (~10%) external current drive capability to be used for control. In such plasmas the current and pressure profiles are tightly coupled because J(r) is entirely determined by p(r) [or more accurately by the kinetic profiles]. The pressure gradient in turn is determined by transport coefficients which depend on the poloidal field profile. Since the dominant energy source will be the internal α-particle heating, the effectiveness of external controls will be limited. The coupling among plasma parameters is illustrated in Fig. 1.

There are several important questions concerning such plasmas: what are the self-consistent profiles of pressure and current; what are the β limits under these conditions and is β sufficient for reactor operation; are these states unique; are these states stable against transient fluctuations; can control methods be devised to maintain optimum conditions? In the experiments reported here we begin to address these issues. These results illustrate the need for development of new control techniques for noninductive, high bootstrap fraction operation of large burning plasmas. While there have been a number of studies of plasmas without transformer induction but far from β limits [1–4], and of essentially 100% noninductive plasmas at higher β but with transformer current control [5,6], this is the first study to explore plasma behavior near the β limits without transformer control or current regulation.

To begin to address these questions, DIII-D experiments with stationary plasmas but without transformer induction have reached $\beta_N \approx \beta_p \approx 3.2$ with ≥ 80% bootstrap current fraction. These conditions have been maintained for > 3.7 s, in plasmas with $I_p \approx 0.6$ MA and $\beta \approx 1.5\%$. The plasmas show intermittent formation of an internal transport barrier (ITB) in all channels (n_e, T_e, T_i, Ω_ϕ). The improved confinement and higher β associated with the ITBs lead to current overdrive (>50 kA/s) arising from the increased bootstrap current. The achievable pressure and current are limited by a relaxation oscillation involving the growth and rapid collapse of the ITB. The recovery of the plasma from these collapse events has

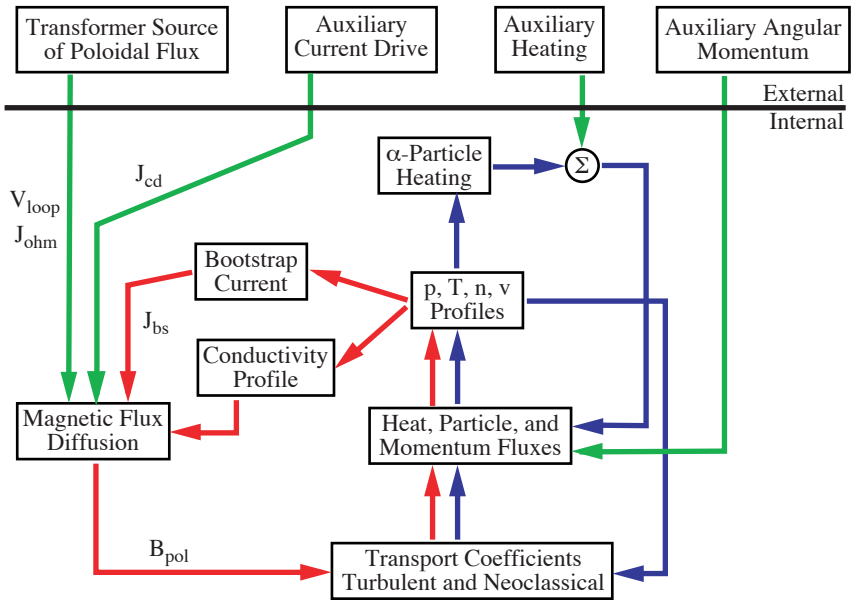

Fig.1. Nonlinear couplings in advanced tokamak transport. The blue lines indicate the fast heat and momentum transport loops, the red lines show the slow magnetic flux transport loop, and the green lines represent external inputs and controls. In small devices the external inputs are dominant, but in a burning plasma the external inputs will be very weak.

positive implications for eventual steady-state operation. The self-consistent plasma state has a broad current profile, with low internal inductance ($l_i \leq 0.6$), no-wall n=1 ideal kink β limit at ~5–6×l_i, and flat or weakly inverted central q (~3), with $q_{95} \sim 10$. Typically, there is 65%–85% bootstrap current, 15%–30% NBCD, and 0%–10% ECCD.

Among the conclusions to be drawn from these experiments is that the noninductive plasma appears to be robust to the ITB relaxation oscillation, repeatedly returning to its previous state. However, because of the pressure and current variation caused by the relaxation oscillation and other transients, a steady-state reactor may need to use a transformer to limit excursions of the total current.

2. Slow Plasma Evolution

These discharges are prepared using the transformer, NBI, and ECH to approximate the expected noninductive profiles. Then the transformer current is held constant, to allow the plasma to relax noninductively. We have worked on development of a voltage feedback control technique to maintain zero voltage at the plasma surface. This has been demonstrated to work in principle, but is not yet generally used. Usually, the NB power is controlled so as to maintain a constant diamagnetic signal. Plasma behavior is very similar with constant NB power, but it is more convenient to set the requested energy or beta. A typical plasma is a high triangularity, symmetric double-null shape, operating in ELMy H-mode, with an initial 650 kA plasma current, and 5–8 MW of auxiliary heating (Fig. 2). In this discharge, the transformer current is held fixed from 1.5 s onward.

During the noninductive phase of this discharge, the plasma parameters continue to evolve. The energy and particle confinement gradually improve, and the current profile broadens. Table 1 compares global parameters early (2.25 s) and late (4.75 s) in discharge 119787, averaged in each case over a 1 s interval.

Note that there is no change in the peaking of the pressure profile, and that the increase in the stored energy is primarily due to the density increase. Current profile broadening is indicated by both the increase in q_{min} and the decrease in l_i. Also notable is the increase in

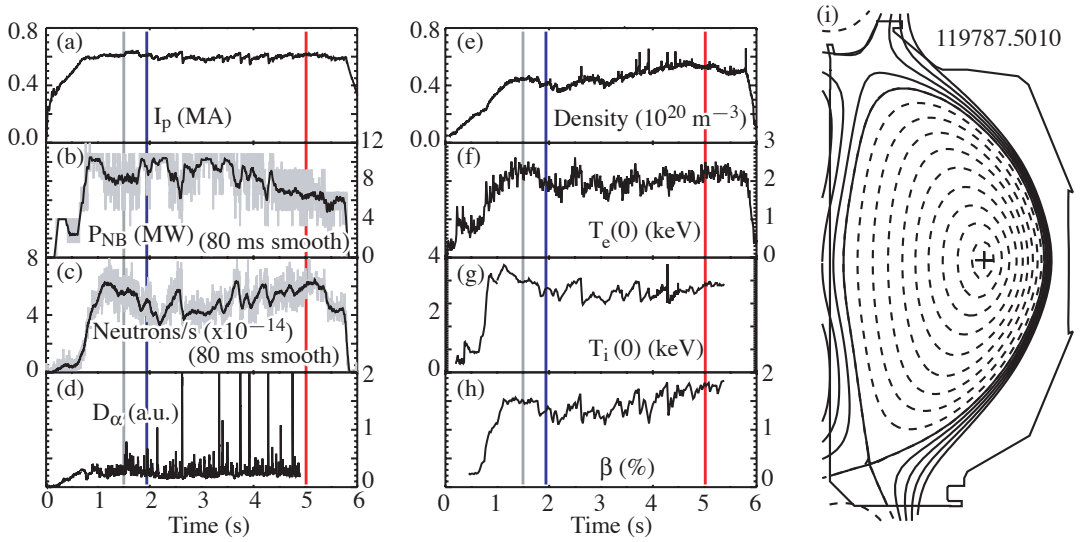

Fig. 2. Overview of discharge 119787. The transformer current is fixed from 1.5 s onward (gray line). (a) plasma current, (b) neutral beam power (80 ms average), (c) neutron rate (80 ms average), (d) D_α light from the divertor, (e) chord-averaged density, (f) central electron temperature, (g) central ion temperature, (h) beta, and (i) equilibrium reconstruction at 5.01 s. The red and blue lines indicate the times for the profiles in Fig. 3.

Table 1.

Parameter	unit	@ 2.25 s	@ 4.75 s	ratio
$\langle n_e \rangle$	10^{20} m^{-3}	0.338	0.437	1.29
$\langle T_e \rangle$	keV	1.41	1.49	1.06
$\langle T_i \rangle$	keV	1.93	2.08	1.08
H_{89P} [7]		1.78	2.73	1.53
H_{98y2} [7]		1.52	2.03	1.34
$p(0)/\langle p \rangle$		2.00	2.02	1.01
β_p		2.55	3.18	1.25
β_N		2.54	3.08	1.21
W	MJ	0.549	0.677	1.23
q_{min}		2.61	2.94	1.13
ℓ_i		0.669	0.563	0.84
τ_E	ms	59.6	97.9	1.64

overall confinement quality. Profiles early and late in the discharge evolution are shown in Fig. 3. At these times there is relatively little transient instability activity in this plasma. The profiles near the end of the discharge do not show the development of a strong transport barrier (see the discussion of Fig. 9, below), but rather the gradient occurs over a wider region. Also, the frequency and amplitude of the ITB relaxation events diminish. Overall the ion thermal conductivity determined from power balance estimates decreases by a factor of about 1.6 during the evolution of the discharge, becoming approximately equal to the ion neoclassical value.

As a result of the increase in stored energy and the decrease in internal inductance, by the end of the discharge $\beta_N \approx 6l_i$ without large-scale instability (Fig. 4). Also, the bootstrap fraction increases from ~0.6 to >0.8 for the final 0.7 s of the discharge (Fig. 5). The contributions to the bootstrap current from n_e, T_e, and T_i gradient terms are approximately in the ratios 35:35:30. The remainder of the current is provided by NBCD, which follows the trend of the injected power. The bootstrap and beam-driven currents account for all of the

current, to within the accuracy of the profile measurements and the models used for calculating the currents. The bootstrap alignment parameter is BSA ≈ 0.65; this is a measure of the rf power needed to drive the difference between the bootstrap and total currents, defined as

$$\mathrm{BSA} = 1 - \left[\int dV \frac{n_e}{T_e} \left| J_{\|} - J_{\mathrm{boot}} \right| \Big/ \int dV \frac{n_e}{T_e} \left| J_{\|} \right| \right] \quad . \tag{1}$$

Where $J_{\|} = \langle \underline{J} \cdot \underline{B} \rangle / B_{TO}$.

The components of the current profile late in the discharge are shown in Fig. 6. The sum of the calculated bootstrap and beam-driven currents closely matches the total. At this time, the total current is 607 kA, the bootstrap current is 523 kA and the beam-driven current is 124 kA. (Total current is measured with a Rogowski coil; bootstrap and beam-driven currents are calculated using measured kinetic profiles.) The sum of the calculated noninductive currents is 647 kA. This 40 kA difference is well within the uncertainty of the calculation.

In order to assess the dependence of the final, noninductive state on the initial conditions, a density scan and a timing scan were carried out. The three discharges illustrated in Fig. 7 were prepared identically except for varying initial density. After freezing the transformer current at 2.0 s,the density and current evolve without control. As indicated the line-averaged electron density, the total current, and the bootstrap

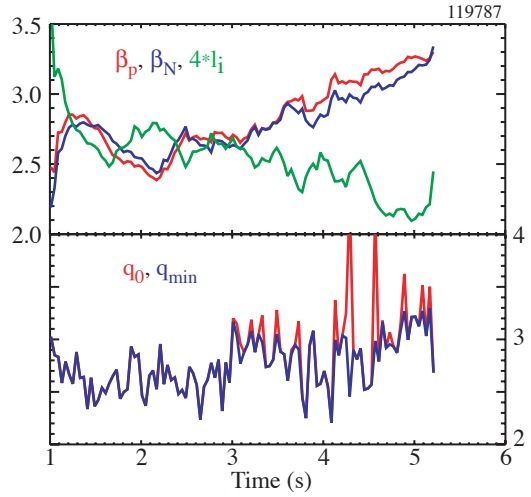

Fig. 4. Evolution of (a) β_p, β_N, and the internal inductance, and (b) q(0) and q_{min}.

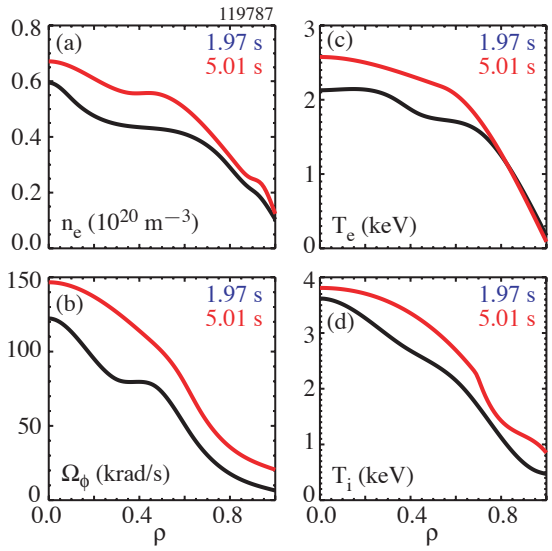

Fig. 3. Profiles of (a) electron density, (b) toroidal rotation, (c) electron temperature, and (d) ion temperature at 1.97 s (early in the discharge evolution; black) and 5.01 s (near the end of the discharge; red).

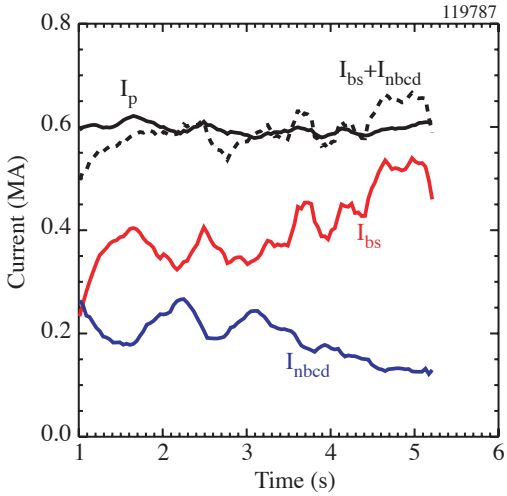

Fig. 5. Time history of the current (0.25 s average); total plasma current (black), bootstrap current (red), beam-driven current (blue), sum of bootstrap and beam-driven currents (black, dash).

current fraction are closely coupled. Increasing the density leads to a much higher bootstrap fraction and to a reduction in the current decay rate. Even small variations in the density and current are correlated. There is an increase in bootstrap fraction whenever the density rises or remains constant for an interval.

3. Fluctuations and Oscillations

The current and stored energy in these discharges does not vary smoothly in time. As illustrated in Fig. 8, the current and the energy follow a saw-tooth-like pattern, with intervals of rising energy and current, indicating good confinement and current overdrive, interspersed with rapid drops. Typically the size of these oscillations (peak-to-peak) is of the order of 10% in current and 20% in energy.

This relaxation oscillation is at present the limiting process for beta and the bootstrap current. As indicated in Fig. 8, trying to increase the average pressure and bootstrap current by increasing the injected power leads to an increase in the frequency of the relaxation events. The process occurring here is the repetitive build-up and collapse of an internal transport barrier (ITB) at large minor radius. The profiles shown in Fig. 9 illustrate this process. At 3.9 s, just prior to the collapse, the T_e and T_i profiles show a narrow region of large gradient at $\rho \approx 0.75$. There are also steep gradients in n_e and Ω_ϕ, but not as pronounced. Just after the collapse, the temperatures have fallen in the outer half of the plasma, the density profile has broadened, and the rotation has decreased throughout. The narrow peak in the bootstrap current has been eliminated. Just before the next collapse, at 4.25 s, all of the profiles have returned to the values at 3.9 s. During the interval between 3.925 s and 4.25 s, the ion thermal conductivity estimated from power balance decreases linearly, by a factor of about two.

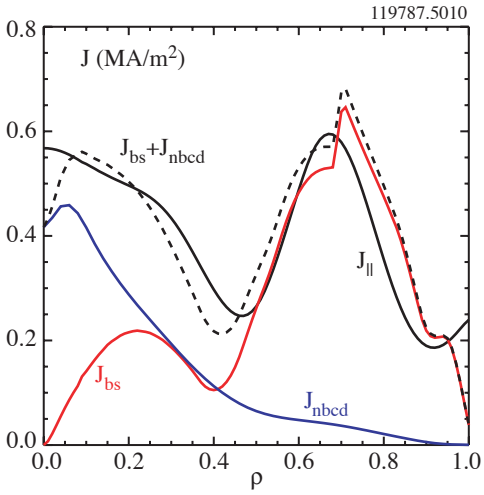

Fig. 6. Current profiles for discharge 119787 at 5.01 s: total (black) from EFIT, bootstrap (red), NBCD (blue), and the sum of J_{bs} and J_{nbcd} (black, dash) calculated from kinetic profiles (see Fig. 3).

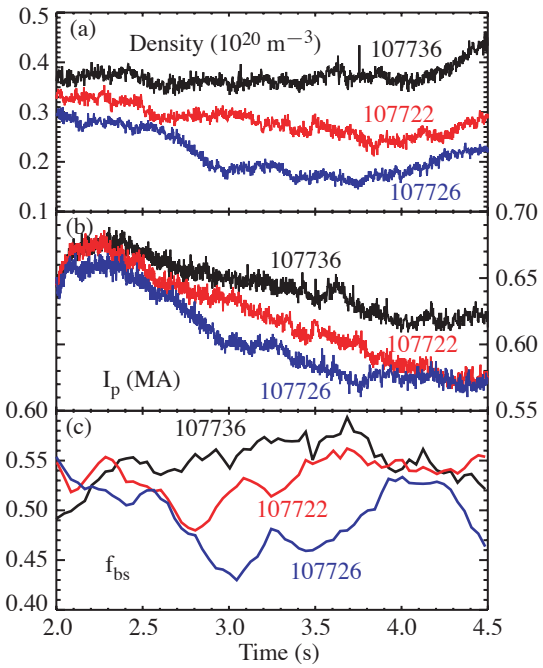

Fig. 7. Three discharges prepared with different initial densities. The transformer current is fixed at 2.0 s. (a) line-average density (CO_2 interferometer); (b) total current; (c) bootstrap current fraction (160 ms average).

The ITB collapse has many similarities to a very large ELM. The expelled density and energy is seen in the SOL, and there is a burst of D_α light from the divertor region similar in shape to an ELM. The signature of this event on the Mirnov loops is indicative of a very fast MHD instability, lasting only 100–300 μs. Analysis of linear ideal MHD stability using the

GATO code indicates that the plasma is very close to an n=1 instability, with a mode pattern reminiscent of the peeling-ballooning modes usually associated with ELMs. The principal difference is that the largest poloidal component is located at $\rho \approx 0.7$, near the region of maximum pressure gradient. Figure 10 shows the quantity $\xi \cdot \nabla \psi$, proportional to the total displacement, versus normalized poloidal flux. The total displacement on the outboard side peaks at the boundary, similar to large ELMs in high performance H-modes [8].

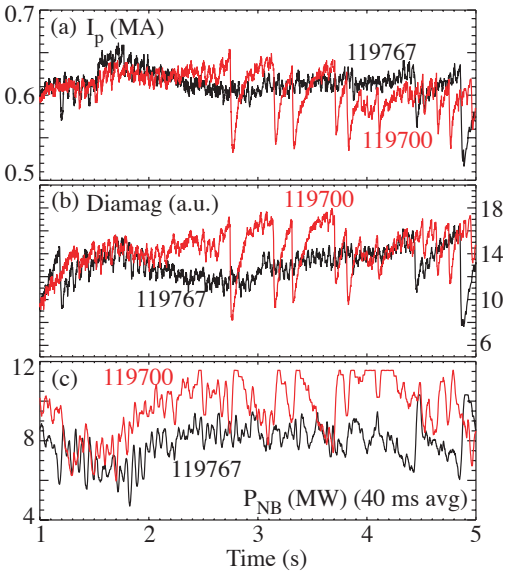

Fig. 8. Frequency of relaxation events increases as plasma energy and injected power and plasma energy are increased. Discharges 119767 (black) and 119700 (red). (a) plasma current, (b) diamagnetic loop signal, (c) neutral beam power.

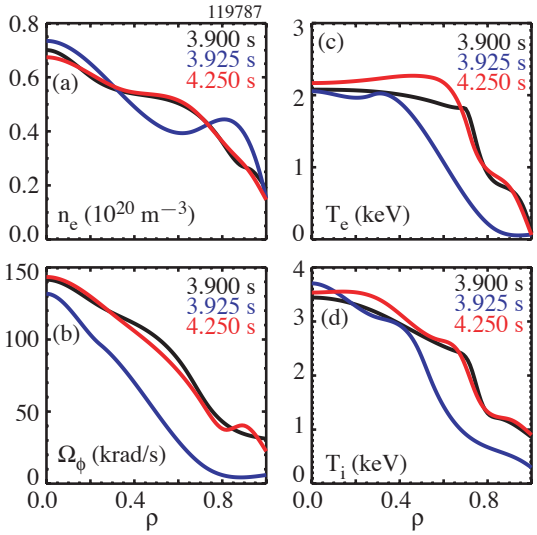

Fig. 9. Profiles of (a) electron density, (b) toroidal rotation, (c) electron temperature, and (d) ion temperature just before an ITB collapse (3.9 s, black), just after the collapse (3.925 s, blue), and just before the next ITB collapse (4.25 s, red).

4. Summary and Conclusions

Some answers to the questions posed in the introduction to this paper are beginning to emerge. In many respects they encourage optimism about the prospects for fully noninductive, bootstrap-driven tokamak operation. The self-consistent profiles of pressure and current are broader than is ordinarily encountered in pulsed tokamak operation. The normalized beta level reached is comparable to other scenarios ($3<\beta_N<4$), but with $\beta_N \sim 6l_i$. The limiting instability is associated with a relaxation oscillation involving the repetitive growth and collapse of an ITB at large minor radius. The MHD mode which triggers the collapse has a peeling-ballooning character with peak amplitude at the radius of maximum pressure gradient, near the edge. A very optimistic observation is that these plasmas recover from the large transient fluctuations due to the ITB collapse and return to essentially the same configuration.

Whether this state is unique, and whether this dynamic stability persists is the subject of future study. For the limited conditions studied thus far, it appears that there is a single state the plasma is evolving toward (Fig. 11). Also for future study is the beta level which can ultimately be achieved in fully bootstrapped plasmas. To provide an interesting value of β (~4%) for a reactor, q_{95} would have to be reduced by a factor of at least two. Although $\beta_N H_{89} > 8$ in the present cases, $\beta_N H_{89}/q^2$ is ~ 0.1, a factor of 4-5 below the ITER baseline value. That the maxima of the current density and the pressure gradient are located near the edge gives some encouragement to the application of edge and wall mode control systems now being developed to improving the stability of these plasmas. Finally, the fluctuating character of the high β noninductive state indicates that

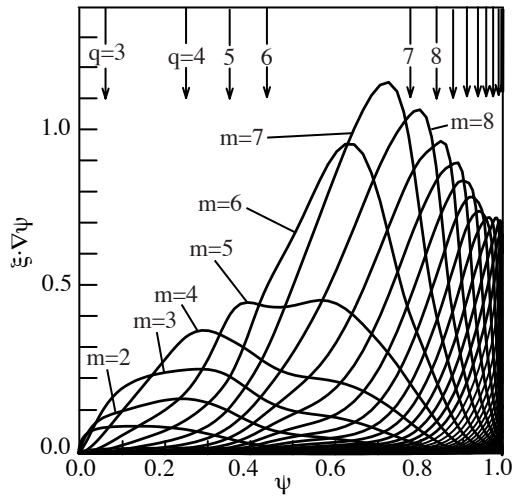

Fig. 10. The ideal n=1 mode structure for the profiles at 5.01 s in discharge 119787 (see Fig. 3).

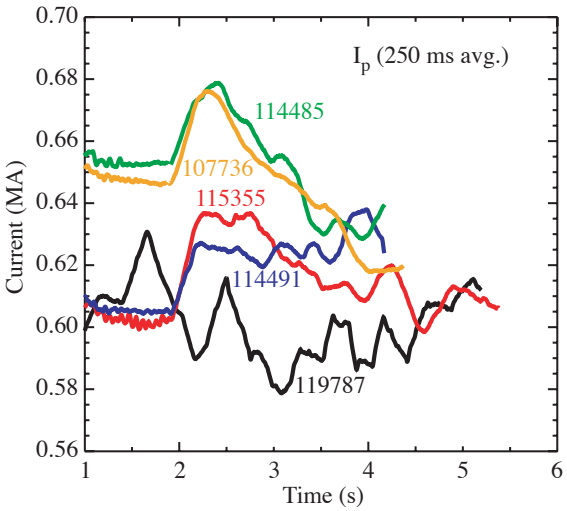

Fig.11. Plasma current vs. time for five different discharges. The indication is that, until the heating power pulse ends, these are all trending toward roughly the same level.

the transformer may have to be used as a control tool to maintain steadier current. This will entail the capability of noninductive overdrive, in order to recharge the transformer and maintain zero average flux change.

Acknowledgment

Work supported by U.S. Department of Energy under Contracts DE-FC02-04ER54698, DE-AC05-96OR22464, DE-AC02-76CH03073, W-7405-ENG-48, and Grants DE-FG02-04ER54758 and DE-FG03-86ER53225.

References

[1] MOREAU, D., *et al.*, Phys. Fluids **B 4** (1992) 2165; SAUTER, O., *et al.*, Phys. Rev. Letters **84** (2000) 3322; SAUTER, O., *et al.*, Phys. Plasmas **8** (2001) 2199; HENDERSON, M.A., *et al.*, Phys. Plasmas **10** (2003) 1796.

[2] HOANG, G.T., *et al.*, Phys. Rev. Lett. **90** (2003) 155002.

[3] ZUSHI, H., *et al.*, Nucl. Fusion **43** (2003) 1600.

[4] LITAUDON, X., *et al.*, Nucl. Fusion **43** (2003) 565.

[5] OIKAWA, T., *et al.*, Nucl. Fusion **40** (2000) 435; KAMADA, Y., *et al.*, Nucl. Fusion **41** (2001) 1311; FUJITA, T., *et al.*, Phys. Rev Lett. **87** (2001) 085001; IDE, S., *et al.*, Plasma Phys. Control. Fusion **44** (2002) L63 (2002).

[6] HOBRIK, J., *et al.*, Phys. Rev. Lett. **87** (2001) 085002; WOLF, R.C., *et al.*, Nucl. Fusion **41** (2001) 1259.

[7] ITER Physics Basis, Nucl. Fusion **39** (1999) 2175.

[8] TURNBULL, A.D., et al., Plasma Phys. and Control. Fusion **45** (1999) 2175.